HOSTED BY
ELSEVIER
CrossMark
Available online at www.sciencedirect.com
ScienceDirect
Progress in Natural Science: Materials International 26 (2016) 49–57
Progress in Natural Science Materials International
www.elsevier.com/locate/pnsmi
www.sciencedirect.com

Original Research

Effect of Y_2O_3 content in the pack mixtures on microstructure and oxidation resistance of B–Y modified silicide coating

Yanxiang Liu, Wan Wang, Zongjie Liu, Chungen Zhou*

School of Materials Science and Engineering, Beijing University of Aeronautics and Astronautics, Beijing 100191, China

Received 24 August 2015; accepted 1 September 2015
Available online 11 February 2016

Abstract

B–Y modified silicide coatings were prepared on Nb–Si based alloy by pack cementation at 1300 ℃ for 10 h. The effect of Y_2O_3 content in the pack mixtures on microstructure and oxidation resistance of the coatings was investigated. The results show that the four coatings have similar structures, which possess a $(Nb,X)Si_2$ outer layer and a $(Nb,X)_5Si_3$ transitional layer. Y_2O_3 content in the pack mixtures has an obvious effect on the Si content in the coating. The mass gains of the coatings prepared with 0.5, 1, 2 and 3 wt% Y_2O_3 in pack mixtures are 2.33, 1.96, 2.05 and 2.86 mg/cm^2 after oxidation at 1250 ℃ for 100 h, respectively. The coating prepared with 1 wt% Y_2O_3 exhibits the best oxidation resistance due to the formation of a dense glass-like borosilicate scale.

Keywords: Coating; High-temperature alloys; Intermetallics; Oxidation

1. Introduction

Niobium silicide based alloys have attracted much attention as candidates for high temperature structural materials because of their high melting points, low density and high strength at high temperatures [1–3]. However, the widespread application of Nb–Si based materials is still limited due to their poor oxidation resistance at elevated temperatures. Alloying can enhance the oxidation resistance of Nb alloys, but simultaneously it degrades the mechanical properties [3–7]. Thus, in order to be used at high temperatures in air, Nb–Si based alloys need to be coated with oxidation-resistant materials [8–10].

An oxidation-resistant coating must serve as a barrier against oxygen penetration and form a dense, adherent and slow-growing oxide scales. Silicide and aluminide coatings on Nb–Si based alloys were found to be suitable for improving their high-temperature oxidation performance by forming the protective oxide scales such as SiO_2 and Al_2O_3, respectively [9–14]. Specially, silicide coatings can offer relative good oxidation resistance at high temperatures due to the formation of amorphous SiO_2 scale, which may flow and heal cracks [15]. However, there are two major factors limiting the long-term application of silicide coating at high temperature. Firstly, the high viscosity of SiO_2 results in reducing the ability to heal the pores and cracks at high temperature. Fortunately, Perepezko et al. have studied that adding B to silicide coatings can improve the oxidation resistance of the coatings by lowering the scale viscosity [8,16–18]. Secondly, the brittleness of pure silicide coatings hinder their long-term applications seriously. Adding a small amount of active elements, such as Y, Ce and La, etc, to the coatings has proved to be available to refine the grain sizes and modify the brittleness of the coatings, and correspondingly reduce the oxidation rate and improve the adherence of the oxide layer [7,19–23]. Guo et al. showed that Si − Y co-deposition coating had superior oxidation resistance at high temperature [24–26]. Moreover, the addition of Y improved the sintering characteristics and plasticity of the oxides, which reduced the stress in the scale [27].

However, few studies focused on the B–Y modified silicide coating simultaneously. Thus, in this study the B–Y modified silicide coating was prepared on the surfaces of Nb–Si based alloy by pack cementation process. The effects of Y_2O_3

*Corresponding author. Tel.: +86 10 82338622.
E-mail address: cgzhou@buaa.edu.cn (C. Zhou).
Peer review under responsibility of Chinese Materials Research Society.

http://dx.doi.org/10.1016/j.pnsc.2016.01.003

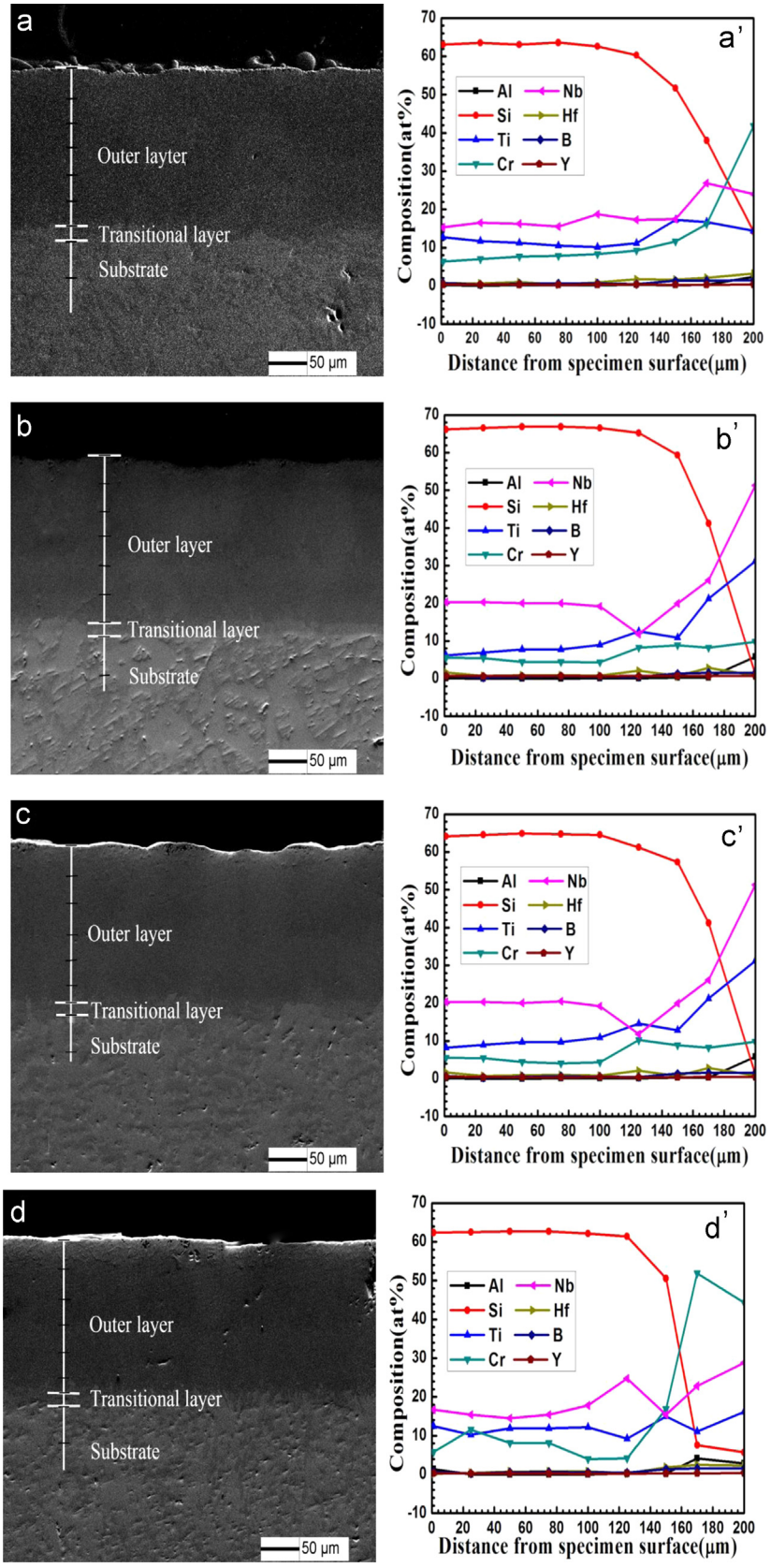

Fig. 1. Cross sectional BSE image and major elemental concentration profiles of B–Y modified silicide coating prepared with pack mixtures containing different mass fractions of Y_2O_3: (a,a′) 0.5%; (b,b′) 1%; (c,c′) 2%; (d,d′) 3%.

Table 1
The compositions of four coatings determined by WDS.

The content of elements (at%)		Si	Ti	Cr	Nb	Hf	Al	B	Y
0.5 wt%	The outer layer	63.07	12.78	6.41	16.51	0.70	0.08	0.11	0.34
Y_2O_3	The transitional laye	41.99	16.68	11.12	24.98	2.08	1.70	0.11	0.34
1 wt%	The outer layer	66.75	7.69	4.07	19.66	0.83	0.12	0.16	0.72
Y_2O_3	The transitional laye	43.23	18.03	8.03	24.91	2.57	2.35	0.16	0.72
2 wt%	The outer layer	64.94	9.43	10.06	14.33	0.52	0.14	0.12	0.46
Y_2O_3	The transitional laye	42.52	18.01	9.03	25.78	1.74	2.34	0.12	0.46
3 wt%	The outer layer	62.50	12.21	9.02	15.50	0.33	0.06	0.09	0.29
Y_2O_3	The transitional laye	40.52	14.91	15.74	24.47	1.84	2.14	0.09	0.29

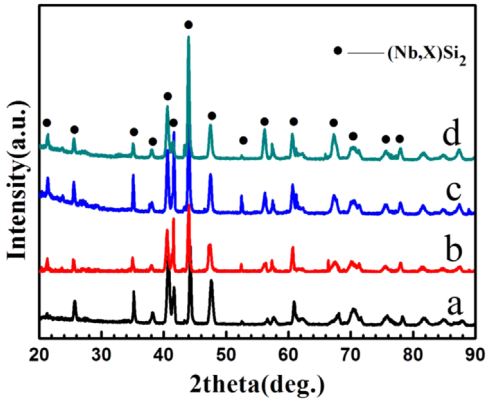

Fig. 2. XRD patterns conducted on the surfaces of the B–Y modified silicide coatings prepared with pack mixtures containing different mass fractions of Y_2O_3: (a) 0.5%; (b) 1%; (c) 2%; (d) 3%.

content on structure and oxidation resistance of the coatings were investigated. The oxidation kinetics was also discussed by analysing the micro-structural and elements composition of the oxide layers formed during the exposure of the alloys at 1250 ℃ in dry static air.

2. Materials and methods

2.1. Specimen preparation

The alloy ingot with a composition of Nb–16Si–22Ti–17Cr–2Al–2Hf (at%) was prepared by vacuum nonconsumable arc melting. To ensure composition homogeneity the alloy was remelted more than five times. After solidification, the ingot was annealed under argon gas atmosphere at 1250 ℃ for 50 h in order to obtain a stable microstructure. For the coating and oxidation experiments, the master alloy ingot was cut into 8 mm × 8 mm × 3 mm cubes by electro-discharge machining. All six sides of each specimen were ground with silicon carbide paper to 800 grits and then ultrasonically cleaned in ethanol.

2.2. Coating process

The Si–B–Y coating applied to alloy specimens was prepared by pack cementation process [16,18]. Pure Si, TiB_2, Y_2O_3, NaF and Al_2O_3 were used as donor sources, halide

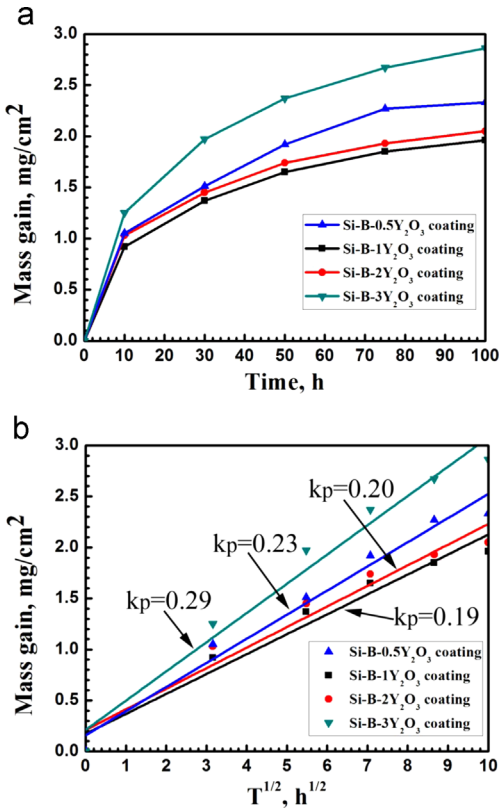

Fig. 3. (a) The oxidation kinetics and (b) linear plot of B–Y modified silicide coatings prepared with different Y_2O_3 content in the pack mixtures after oxidation at 1250 ℃ for 100 h.

activator and inert filter of the pack mixtures respectivety. The powder mixtures composed of $8Si–8TiB_2–xY_2O_3$ ($x=0.5,1,2,3$)–5NaF–$(79-x)Al_2O_3$(wt%). Each kind of powders was weighed according to the ratio and then mixed uniformity. Then, both the well-mixed powders and clean samples were loaded in a cylindrical alumina crucible with dimension of Φ 20 × 35 mm^2 followed by sealing with an alumina lid. After that the pack was loaded under an Ar atmosphere in the furnace chamber. Under a steady flow of argon, the furnace was heated to 1300 ℃ at a rate of 5 ℃ min^{-1} and sustained 10 h, then, cooled down to room temperature naturally. The coated specimens were retrieved from the pack and cleaned in an ultrasonic water bath to remove any residual powders on their surfaces.

2.3. Oxidation tests

The oxidation tests were conducted in static air in an open-ended tube furnace at 1250 ℃ for 100 h. The specimens were taken out of the furnace to cool at room temperature for a weight measurement at intervals of 10, 30, 50, 75, 100 h and then back into the furnace to continue the oxidation tests. The mass gain of these specimens was measured by a precision analytical balance (Model CPA225D, Germany) with an accuracy of 10^{-5} g. Three measurements for weight gain at each time were conducted and the average value was employed.

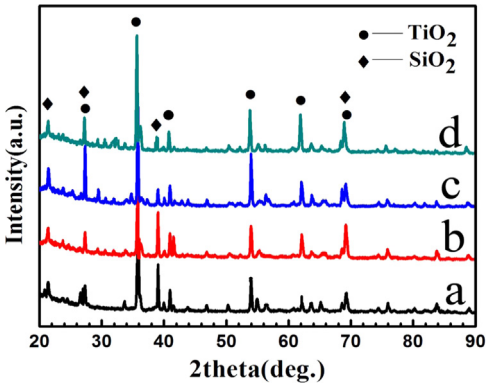

Fig. 4. XRD patterns conducted on the surfaces of the B–Y modified silicide coating prepared with (a) 0.5%, (b) 1%, (c) 2% and (d) 3% (mass fraction) Y_2O_3 content in the pack mixtures after oxidation at 1250 ℃ for 100 h.

2.4. Analyzing method

Both coated and oxidized specimens were analyzed by X-ray diffraction (XRD, Model D/Max 2500PC Rigaku, Japan), scanning electron-microscopy (SEM, Model FEI Quanta600, USA) with energy-dispersive spectroscopy(EDS) and electron microprobe analysis (EPMA, Model JXA-8230, Japan, the spot diameter is 1 μm) with wave dispersive spectroscopy (WDS) to identify the phase constituents, morphology and compositional distribution.

3. Results and discussions

3.1. Microstructure of coating

The cross-sectional microstructures and major elemental concentration profiles are shown in Fig. 1 for B–Y modified silicide coatings prepared with 0.5, 1, 2 and 3 wt% Y_2O_3

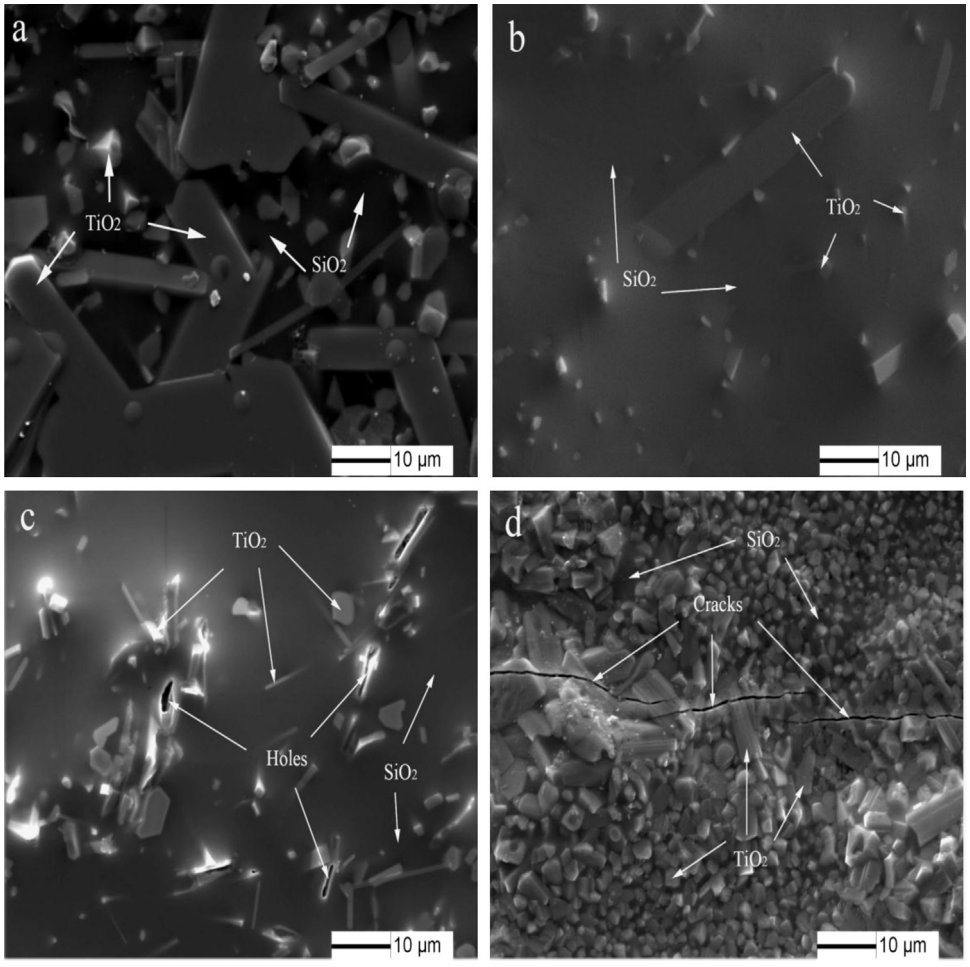

Fig. 5. Surface morphologies of B–Y modified silicide coating prepared with (a) 0.5%, (b) 1%, (c) 2% and (d) 3% (mass fraction) Y_2O_3 content in the pack mixtures after oxidation at 1250 ℃ for 100 h.

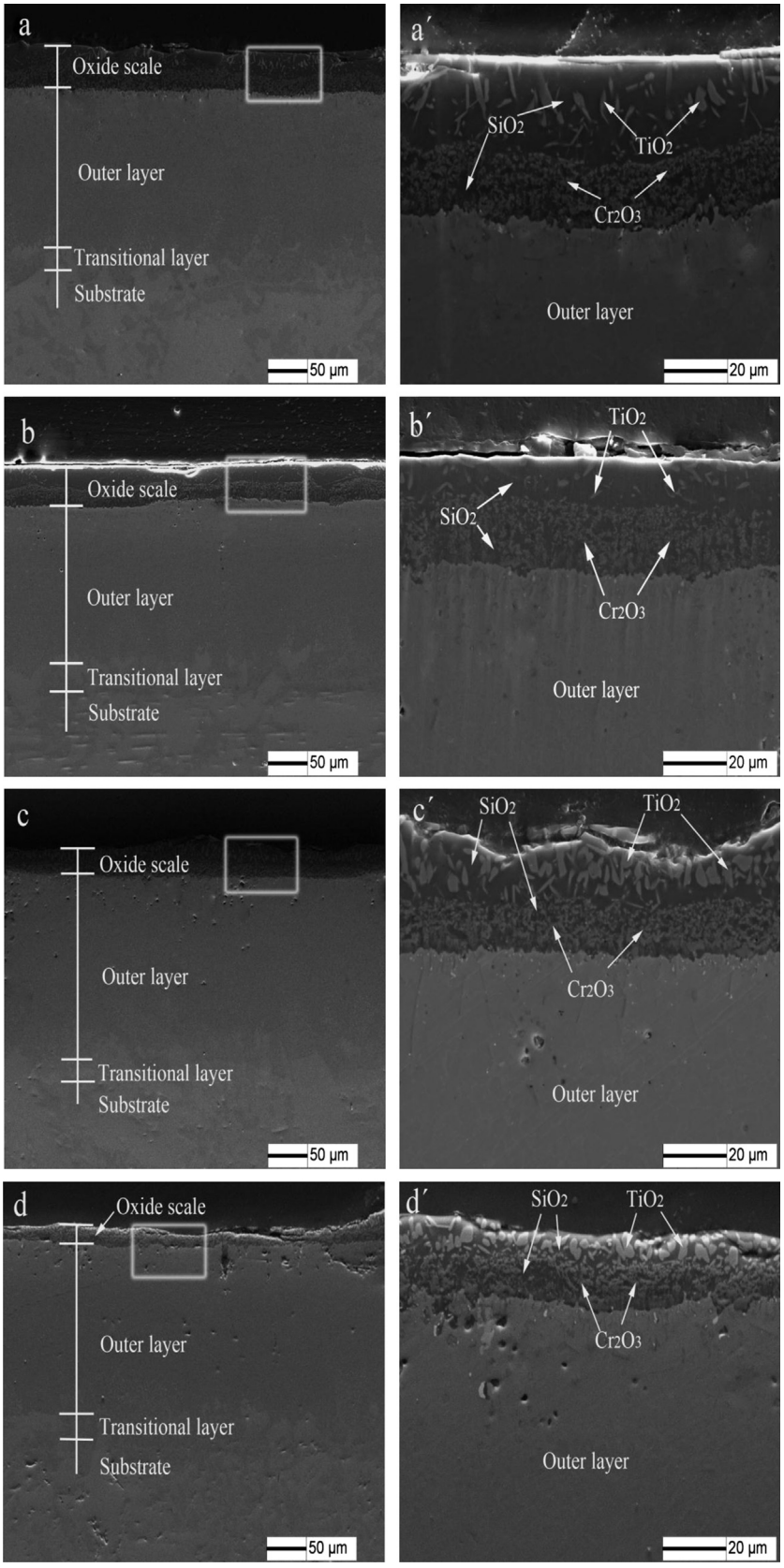

Fig. 6. Cross-sectional SEM images of B–Y modified silicide coating prepared with (a,a′) 0.5%; (b,b′) 1%; (c,c′) 2% and (d,d′) 3% (mass fraction) Y_2O_3 content in the pack mixtures after oxidation at 1250 ℃ for 100 h.

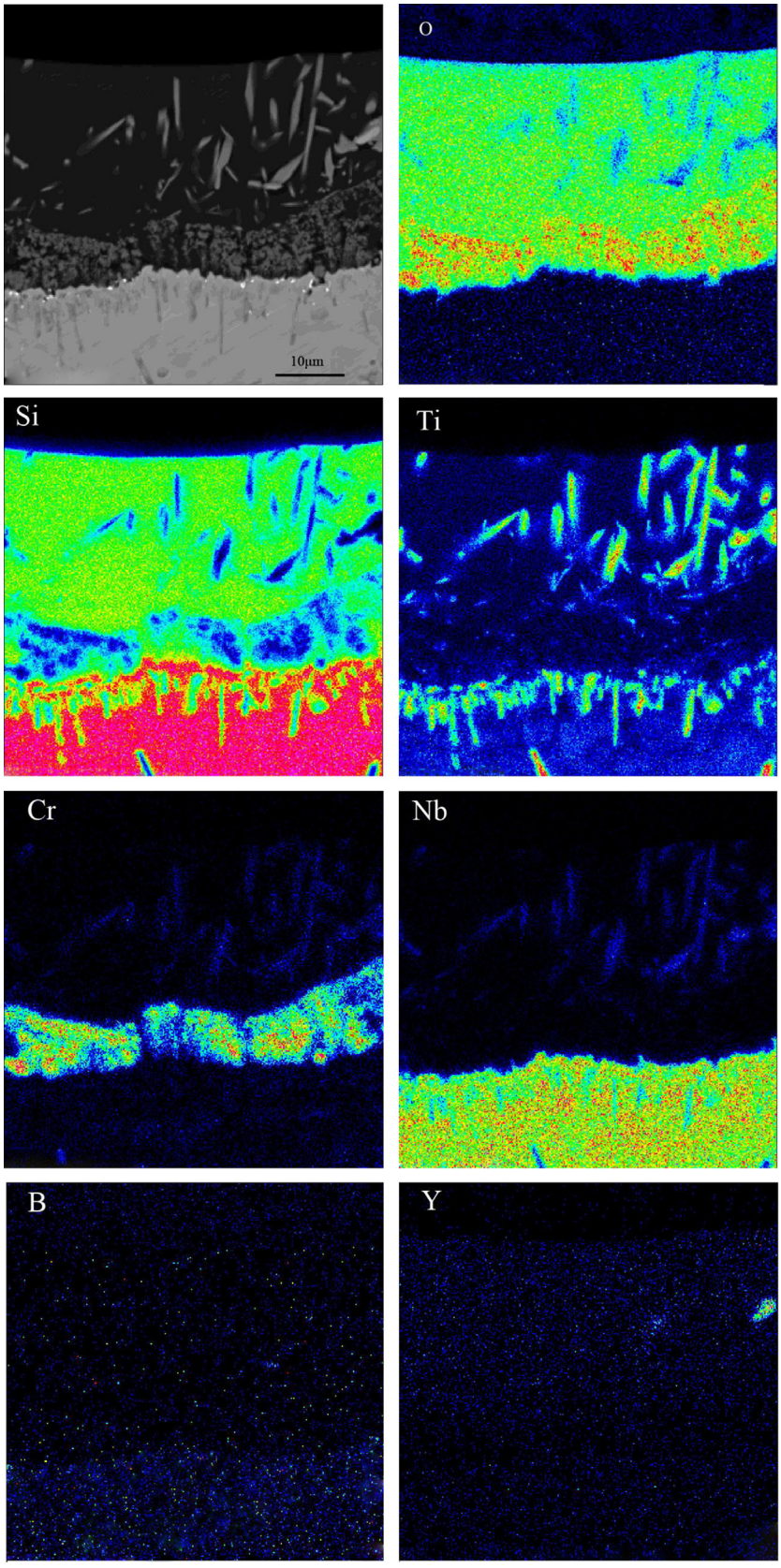

Fig. 7. EPMA elemental mappings for Si–B–Y coating prepared with 1 wt% Y_2O_3 content in the pack mixtures after oxidation at 1250 ℃ for 100 h.

content in the pack mixtures held at 1300 ℃ for 10 h. It can be seen that these four coatings have similar coating structures, which possess an outer layer and a transitional layer. The thicknesses of outer layer and the transitional layer of these four coatings are 160 μm and 11 μm, 168 μm and 15 μm, 163 μm and 13 μm, 154 μm and 10 μm, respectively. It concludes that with increase of Y_2O_3 in the pack from 0.5 to 3 wt%, the thickness of coating increases firstly but then decreases.

The corresponding concentration profiles of the four coatings, obtained by WDS, are shown in Fig. 1(a′)–(d′). The element composition of the outer layer and the transitional layer for the four coatings is listed in Table 1. The compositional values are the average values of the composition for each point in Fig 1(a′)–(d′). As can be seen, a small quantity of B disperses uniformly in the four coatings with a concentration of 0.11, 0.16, 0.12 and 0.09 at%, respectively. And the Y disperses uniformly in the four coatings with a concentration of 0.34, 0.72, 0.46 and 0.29 at%, respectively. Besides, with the addition of 0.5, 1, 2 and 3 wt% Y_2O_3 content in the pack mixtures, the content of Si in the coating is 63.07, 66.75, 64.94 and 62.50 at%, respectively. Thus, with the increase of Y_2O_3 content in the pack mixtures from 0.5 to 3 wt%, the content of Si in the coating increases firstly but then decreases. The content of Si in the coating prepared with 1 wt% Y_2O_3 content in the pack mixtures is maximum. Furthermore, Al_2O_3 is not found in these four coatings, suggesting that the coatings grow predominantly by the inward diffusion of Si, B and Y [26,27].

The X-ray diffraction (XRD) (Fig. 2) shows that the outer layers of four coatings are detected to be composed of (Nb,X) Si_2(X presents Ti, Cr and Hf elements). There is no B-containing and Y-containing phase detected by the XRD. However, through the EPMA major elemental concentration profiles, we can see that B and Y are finely dispersed in the coating and the corresponding concentration is 0.16 and 0.72 at% as analysed by WDS. So we conclude that B and Y exist in form of solid solution in the coatings.

3.2. Static oxidation behavior

The oxidation performance of the coatings was studied at 1250 ℃ for 100 h, and Fig. 3a presents the oxidation kinetics data for B–Y modified silicide coatings prepared with different Y_2O_3 content in the pack mixtures (mass fraction). The mass gains of the coatings prepared with 0.5, 1, 2 and 3 wt% Y_2O_3 content in the pack mixtures are 2.33, 1.96, 2.05 and 2.86 mg/cm^2, respectively. We can conclude that the Si–B–Y coatings perform good oxidation resistance. The oxidation kinetic of the Si–B–Y coated samples follows the parabolic rate law as can be seen in Fig. 3(a). Fig. 3(b) presents the corresponding linear plot of Si–B–Y coated samples. The parabolic rate constants were calculated according to the equation.

$$\left(\Delta m/A\right)^2 = K_p t \quad (1)$$

where Δm is the weight change of the specimen, A is the surface area and t is the exposure time. The parabolic rate constants ($mg^2\,cm^{-4}\,h^{-1}$) of the coatings prepared with 0.5, 1, 2 and 3 wt% Y_2O_3 content in the pack mixtures were 5.29×10^{-2}, 3.61×10^{-2}, 4×10^{-2} and 8.41×10^{-2}, respectively. It is concluded that with the increase of Y_2O_3 content in the pack mixtures from 0.5 wt% to 3 wt%, the mass gain of the coatings after oxidation at 1250 ℃ for 100 h and the parabolic rate constants present a down and then up trend. The coating prepared with 1 wt% Y_2O_3 content in the pack mixtures exhibits the best oxidation resistance.

3.3. Microstructure of oxide scale

The oxidized surfaces of B–Y modified silicide coating were analyzed by XRD (Fig. 4). The main oxides observed after oxidation at 1250 ℃ for 100 h are SiO_2 and TiO_2. Fig. 5 shows the surface morphology of the B–Y modified silicide coatings prepared with 0.5, 1, 2 and 3 wt% Y_2O_3 content in the pack mixtures after oxidation at 1250 ℃ for 100 h. It can be seen that the surfaces mainly consist of a dark glass-like phase and a rod-like phase. EDS analysis on the dark phase reveals that the dark phase has a composition of 61.51O–29.20Si–1.52Ti–7.78Al (at%), which indicates that it is SiO_2, while the rod-like phase has a composition of 62.07O–9.84Si–23.61Ti–2.47Cr–2.01Al (at%), which indicates that it is TiO_2. As can be seen from Fig. 5(a)–(d), with the addition of 0.5–1 wt% Y_2O_3 content in the pack mixtures, the content of SiO_2 in the scale increases obviously, while that of TiO_2 decreases. However, with the addition of 1–3 wt% Y_2O_3 content in the pack mixtures, the content of SiO_2 decreases instead, while that of TiO_2 increases obviously. Besides, the morphology of TiO_2 changes from lath-like structure or rod-like shape to graininess as shown in Fig. 5(a)–(d). Moreover, it shows clearly that the scale is dense and no micro-cracks or micro-holes exists on the surface of the coating prepared with 1 wt% Y_2O_3 content in the pack mixtures after oxidation at 1250 ℃ for 100 h and TiO_2 finely embeds in glass-like SiO_2. However, a large number of TiO_2 exposes on the surface of coating prepared with 0.5 wt% Y_2O_3 content in the pack mixtures after oxidation at 1250 ℃ for 100 h. Besides, some micro-holes and micro-cracks present on the surfaces of the coatings prepared with 2, 3 wt% Y_2O_3 content in the pack mixtures after oxidation at 1250 ℃ for 100 h, respectively.

Fig. 6 shows the cross-sectional microstructures of the B–Y modified silicide coating prepared with 0.5, 1, 2 and 3 wt% Y_2O_3 content in the pack mixtures after oxidation at 1250 ℃ for 100 h with low and high magnifications, respectively. As can be seen from Fig. 6(a)–(d), the thickness of the scales is 41.72, 29.27, 34.51 and 19.40 μm, respectively. Compared with the thickness of the scale on the surface of the coating prepared with 1 wt% Y_2O_3 content in the pack mixtures after oxidation at 1250 ℃ for 100 h, that of the scale on the surface of the coating prepared with 3 wt% Y_2O_3 content in the pack mixtures after oxidation at 1250 ℃ for 100 h is much thinner due to the spalling of the oxide and poor adhesion. EDS analysis indicates that the dark glass-like phase has a composition of 69.18O–26.03Si–3.93Ti–0.58Cr–0.28Hf (at%), confirming that the phase is SiO_2, while the lash-like phase

embedded in the glassy matrix phase and grainy phase existed in the bottom of the scale has the composition of 71.54O–23.42Ti–3.30Cr–1.74Hf and 61.54O–33.93Cr–3.25Si–1.28Ti (at%), confirming the formation of TiO_2 and Cr_2O_3. The scales on the surface of the coatings prepared with 0.5, 1 wt% Y_2O_3 content in the pack mixtures after oxidation at 1250 ℃ for 100 h are continuous and compact as can be seen in Fig. 6(a, a′) and (b, b′). The scales have a dual-layer structure, an outer layer consisted of SiO_2 and TiO_2, and an inner layer mainly contained Cr_2O_3 adjacent to the retained coating, which is similar to the scale developed on the Si–B co-deposition coating [16]. The scales on the surface of the coatings prepared with 2–3 wt% Y_2O_3 content in the pack mixtures after oxidation at 1250 ℃ for 100 h have similar structure with the scales on the surface of the coating prepared with 0.5, 1 wt% Y_2O_3 content in the pack mixtures after oxidation at 1250 ℃ for 100 h as can be seen in Fig. 6(a′)–(d′). The oxide scale on the surface of the coating prepared with 2 wt% Y_2O_3 content in the pack mixtures with slight spalling and voids shows poor adhesion as can be seen in Fig. 6(c) and (c′), but it is much better than the coating prepared with 3 wt% Y_2O_3 content in the pack mixtures. The cross-sectional microstructure of the coating prepared with 3 wt% Y_2O_3 content in the pack mixtures is given in Fig. 6(d) and (d′). It shows that obvious cracks and voids in the scale, indicates the poor adhesion of the oxide scale.

The elemental mapping for Si–B–Y coating prepared with 1 wt% Y_2O_3 content in the pack mixtures after oxidation at 1250 ℃ for 100 h is shown in Fig. 7. It can be seen that the upper part of the scale is a mixture oxide of SiO_2 and a small amount of TiO_2, while the lower part of the scale is a mixture oxide of slight SiO_2 and discontinuous Cr_2O_3. Minute quantity of B finely dispersed in the oxide scale, suggesting that the existence of B_2O_3.

4. Discussion

4.1. The effect of Y_2O_3 on formation of Si–B–Y coating

In this paper, we can see that with the increase of Y_2O_3 content in pack mixtures from 0.5 wt.% to 1 wt%, the content of Si and B in the coating and the thickness of coating increase, but with the continuous increase of Y_2O_3 content in pack mixtures from 1 wt% to 3 wt%, the content of Si and B in the coating and the thickness of coating decrease instead. It is concluded that the addition of Y_2O_3 can accelerate the diffusion of Si and B. However, the accelerated effect of RE element Y on the inward diffusion of Si and B exist an optimum concentration range. The effect of the RE element Y on the diffusion of Si and B is discussed from the following aspects.

The formation of the Si–B–Y coating relates to the production of the active Si, B and Y atoms. During the cementation pack process the following chemical reactions probably occur [28,29].

$$Si(s)+xNaF(l)\rightarrow SiF_x(g)+xNa(g) \quad (2)$$

$$TiB_2(s)+2(x+1)NaF(g)\rightarrow 2BF_x(g)+TiF_2(g)+Na(g) \quad (3)$$

$$Y_2O_3(s)+6NaF(g)\rightarrow 2YF_3(g)+3Na_2O(s) \quad (4)$$

$$2YF_3(g)\rightarrow 2[Y](s)+3F_2(g) \quad (5)$$

$$x[Y](s)+3SiF_x(g)\rightarrow xYF_3(g)+3[Si](s) \quad (6)$$

$$[Y](s)+BFx(g)\rightarrow YFx(g)+[B](s) \quad (7)$$

where x is 1,2,3,4.

At the beginning, the SiF_x and BF_x are formed by the chemical reaction (2) and (3). YF_3 is produced through the chemical reaction (4). Subsequently, YF_3 decompose to active Y atoms according to reaction (5). Then active Y atoms react with SiF_x and BF_x, which produces YF_3 and contributes to liberate active Si and B atoms as can be seen from the chemical reaction (6) and (7). In this way, the concentration of active Si and B atoms on the surface is considerably elevated. Therefore, the inward diffusion of Si and B is accelerated driven by the concentration gradient of atoms.

A thin active Y atoms layer adsorbs on the surfaces of samples with addition of 1 wt% Y_2O_3 content in the pack mixtures. Thus the Y atoms can diffuse into the substrate owing to the concentration gradient. The Y atoms diffused into substrate induces lattice distortion due to the big size, thereby increasing the dislocation density, which provides more diffusion channels for the inward diffusion of Si and B atoms. Therefore, the diffusion rate of Si and B atoms is accelerated obviously. Consequently, a thicker coating is obtained in Fig. 1b.

However, the active atoms Y generated in the pack are too little to produce enough driving force for its diffusion in the coating with addition of 0.5 wt% Y_2O_3 content in the pack mixtures. Thus the lower Y atoms are penetrated to the coatings. When the addition of Y_2O_3 content in the pack mixtures increases to 2–3 wt%, the active Y atoms layer on the surfaces of specimens become thicker. The Y atoms stacked on the surfaces of samples hinder the inward diffusion of Y atoms. Thus, the diffusion of Y atoms in the atom packing layer needs to overcome more resistance. Although the active atoms Y in the pack are numerous, the content of Y penetrated to the coatings decreases. Accordingly, the dislocation density and the quantity of diffusion channels for the inward diffusion of Si and B atoms decrease. The diffusion resistance of Si and B atoms increases due to the concentration of Y atoms on the surface of the specimen. Thereby, the content of Si and B in the coating decreases. As a result, a thin coating is obtained as we can see in Fig. 1(a), (c) and (d). Li et al. investigated effect of Y_2O_3 on Si–Al–Y co-deposition coatings prepared on Ti–Al alloy. They found that the coating thickness and density increased firstly but then decreased when the content of Y_2O_3 in the pack mixtures increased from 1 to 5 wt% [25]. Other similar investigations were also conducted in recent years [30–32].

4.2. Oxidation mechanism of the Si–B–Y coating

We can conclude that the B–Y modified silicide coatings on the alloy Nb–16Si–22Ti–17Cr–2Al–2Hf (at%) have significantly beneficial effect on high temperature oxidation resistance. The oxidation resistance of Si–B–Y coating prepared with 1 wt% Y_2O_3 content in the pack mixtures is superior to that of coatings

prepared with 0.5, 2, 3 wt% Y_2O_3 content in the pack mixtures after oxidation at 1250 ℃ for 100 h in this paper. The main reasons are as follows.

According to the ΔG_0–T plots (Ellingham–Richardson Chart) of various oxides [33,34], the standard free energies for formation of these oxides at 1250 °C are in the following sequence: $\Delta G^0_{TiO_2} < \Delta G^0_{SiO_2} < \Delta G^0_{B_2O_3} < \Delta G^0_{Cr_2O_3}$. Therefore, Ti would be oxidized preferentially to form loose TiO_2 rods. As oxidation is processed, Si is oxidized to SiO_2, and then the as-formed TiO_2 rods are wrapped in glass-like SiO_2, forming dense and mixed scales mainly consisted of SiO_2 and TiO_2. The content of Si atoms penetrated to the coatings prepared with addition of 0.5 wt%, 1 wt%, 2 wt% and 3 wt% Y_2O_3 content in the pack mixtures are 63.07, 66.75, 64.94 and 62.50 at%, respectively. Thus, the coating prepared with 1 wt% Y_2O_3 content in the pack mixtures is more easily to form SiO_2. As the oxygen continually diffuses into the coating, B is oxidized to B_2O_3, which dispersed in the scale. Then, the as-formed SiO_2 reacts with B_2O_3 to form a borosilicate scale, which may flow and heal cracks. Thus, the formation of borosilicate scale is beneficial for the oxidation resistance. Recently, Li also reported that B_2O_3 oxidised from B-modified SiC layer could seal cracks at intermediate temperatures, resulting in improving the oxidation resistance of the coating [35].

Therefore, the coating prepared with 1 wt% Y_2O_3 content in the pack mixtures exhibits the best oxidation resistance due to the formation of a dense glass-like borosilicate scale.

5. Conclusion

The Si–B–Y coatings were prepared with 0.5, 1, 2, 3 wt% Y_2O_3 content in the pack mixtures on Nb–Si based alloy by pack cementation method at 1300 ℃ for 10 h. The results show that the four coatings have similar structures, which possess a (Nb,X)Si_2 outer layer and a $(Nb,X)_5Si_3$ transitional layer. The content of Si and B in the coating and the thickness of coating increase firstly but then decrease with the addition of Y_2O_3 content in the pack mixtures increased from 0.5 to 3 wt%.

The mass gains of the B–Y modified silicide coatings prepared with 0.5, 1, 2 and 3 wt% Y_2O_3 content in the pack mixtures were 2.33, 1.96, 2.05 and 2.86 mg/cm^2 after oxidation at 1250℃ for 100 h, respectively. The oxides mainly consist of SiO_2, TiO_2 and Cr_2O_3. The coating prepared with 1 wt% Y_2O_3 content in the pack mixtures exhibits the best oxidation resistance due to the formation of a dense glass-like borosilicate scale.

Acknowledgements

This project is supported by the National Natural Science Foundation of China under the Contract of 51171010 and 51431003, the Joint Funds of the National Natural Science Foundation of China (U1435201).

References

[1] B.P. Bewlay, M.R. Jackson, J.C. Zhao, P.R. Subramanian, Metall. Mater. Trans. A 34 (2003) 2043–2052.
[2] D.Z. Yao, R. Cai, C.G. Zhou, J.B. Sha, H.R. Jiang, Corros. Sci. 51 (2009) 364–370.
[3] A. Vazquez, S.K. Varma, J. Alloy. Compd. 509 (2011) 7027–7033.
[4] J. Geng, P. Tsakiropoulos, Intermetallics 15 (2007) 382–395.
[5] K. Zelenitsas, P. Tsakiropoulos, Mater. Sci. Eng.: A 416 (2006) 269–280.
[6] J. Wang, X.P. Guo, J.M. Guo, Chin. J. Aeronaut. 22 (2009) 544–550.
[7] X. Song, L. Wang, Y. Liu, H.P. Ma, Prog. Nat. Sci.: Mater. Int. 21 (2011) 227–235.
[8] L.F. Su, O. Lu-Steffes, H. Zhang, J.H. Perepezko, Appl. Surf. Sci. 337 (2015) 38–44.
[9] X.L. Tu, H. Peng, L. Zheng, W.Y. Qi, J. He, H.B. Guo, S.K. Gong, Appl. Surf. Sci. 325 (2015) 20–26.
[10] S. Knittel, S. Mathieu, L. Portebois, S. Drawin, M. Vilasi, Surf. Coat. Technol. 235 (2013) 401–406.
[11] S. Mathieu, N. Chaia, M. Le Flem, M. Vilasi, Surf. Coat. Technol. 206 (2012) 4594–4600.
[12] J.H. Yan, Y. Wang, L.F. Liu, Y.M. Wang, Appl. Surf. Sci. 320 (2014) 791–797.
[13] S. Majumdar, A. Arya, I.G. Sharma, A.K. Suri, S. Banerjee, Appl. Surf. Sci. 257 (2010) 635–640.
[14] B.F. Yuan, Y. Li, M. Qiao, C.G. Zhou, Prog. Nat. Sci.: Mater. Int. 23 (2013) 198–204.
[15] S. Majumdar, J. Kishor, B. Paul, R.C. Hubli, J.K. Chakravartty, Corros. Sci. 95 (2015) 100–109.
[16] Y.Q. Qiao, Z. Shen, X.P. Guo, Corros. Sci. 93 (2015) 126–137.
[17] A. Lange, M. Heilmaier, T.A. Sossamann, J.H. Perepezko, Surf. Coat. Technol. 266 (2015) 57–63.
[18] B.V. Cockeram, Surf. Coat. Technol. 76-77 (1995) 20–27.
[19] A. Rahmel, M. Schiitze, Oxid. Met. 38 (1992) 255–266.
[20] W.H. Yu, J. Tian, W. Tian, J. Zhao, Y.Q. Li, Y.Z. Liu, J. Rare Earths 33 (2015) 221–226.
[21] X. Li, X.P. Guo, Y.Q. Qiao, Oxid. Met. 83 (2014) 253–271.
[22] P. Zhang, X.P. Guo, Surf. Coat. Technol. 206 (2011) 446–454.
[23] Y.T. Liu, X.P. Guo, Prog. Nat. Sci.: Mater. Int. 23 (2013) 190–197.
[24] X.D. Tian, X.P. Guo, Surf. Coat. Technol. 204 (2009) 313–318.
[25] Y.Q. Li, F.Q. Xie, X.Q. Wu, X. Li, Appl. Surf. Sci. 287 (2013) 30–36.
[26] P. Zhang, X.P. Guo, Corros. Sci. 53 (2011) 4291–4299.
[27] R.J. Chrstensen, V.K. Tolpygo, D.R. Clarke, Acta Mater. 45 (1997) 1761–1766.
[28] M. Li, L.X. Song, J. Le, X.P. Song, Z.C. Guo, J. Inorg. Mater. 3 (2005) 764–768.
[29] D.L. Ye, J.H. Hu, Metallurgical Industry Press Beijing, China, 2002.
[30] T. Qi, X.P. Guo, J. Mater. Eng. 1 (2010) 12–18.
[31] T. Qi, X.P. Guo, J. Inorg. Mater. 24 (2009) 1119–1225.
[32] J.T. Guo, C. Yuan, J.S. Hou, Effects of rare earth elements on NiAl-based alloys, Acta Met. Sin. 44 (2008) 513–520.
[33] I. Barin, Thermochemical Data of Pure Substances, third ed, Weinheim, New York, 1995.
[34] M.S. Li, High Temperature Corrosion of Metal, Metallurgy Industry Press, Beijing, 2001, p. 4.
[35] T. Feng, H.J. Li, X.H. Shi, X. Yang, Y.X. Li, X.Y. Yao, Corros. Sci. 60 (2012) 4–9.